Med Chem Res (2016) 25:2015–2029
DOI 10.1007/s00044-016-1660-5

MEDICINAL CHEMISTRY RESEARCH

ORIGINAL RESEARCH

Synthesis, characterization, drug-likeness properties and determination of the in vitro antioxidant and cytotoxic activities of new 1,3,4-oxadiazole derivatives

Nafal Nazarbahjat[1,2] · Azhar Ariffin[1] · Zanariah Abdullah[1] · Mahmood Ameen Abdulla[3] · John Kwong Siew Shia[4] · Kok Hoong Leong[5,6]

Received: 27 July 2015 / Accepted: 4 July 2016 / Published online: 21 July 2016

Abstract A series of new 1,3,4-oxadiazole derivatives were synthesized and evaluated for their antioxidant, cytotoxic, and apoptosis activities. Antioxidant activity was determined in vitro using free radical scavenging (2,2-diphenyl-1-picrylhydrazyl) and ferric reducing antioxidant power assays. Most of the synthesized compounds exhibited significant antioxidant activities. Compound **3** showed the most potent antioxidant activity, comparable to the antioxidants used as positive controls—quercetin, BHT, trolox, rutin, and ascorbic acid. Compound **1** displayed high radical scavenging activity in the 2,2-diphenyl-1-picrylhydrazyl assay, with an half-maximum inhibitory concentration (IC_{50}) = 2.22 ± 0.01 μg/mL. Cytotoxic activities were evaluated in vitro against three human cancer cell lines (BxPC-3, MCF-7, MDA-MB-231) and one normal cell line (hTERT-HPNE) using the MTT assay. Compound **4e** showed the most potent cytotoxic activity against MDA-MB-231 (IC_{50} = 21.40 ± 1.22 μM), and compound **4c** showed the most potent activity against BxPC-3 (IC_{50} = 26.17 ± 1.10 μM). Further investigation on BxPC-3 cells showed compound **4c** induces apoptosis and cell cycle arrest at G0/G1 phase. The drug-likeness parameters of these oxadiazole derivatives were evaluated according to the Lipinski rule, the Veber rule, and Egan's model. All of the derivatives were found to have good predicted absorption characteristics, with the exception of compound **4d** due to its high lipophilicity.

Keywords 1,3,4-oxadiazole · Schiff bases · Drug-likeness properties · Antioxidant activity · Cytotoxic activity · Apoptosis

Abbreviations

BDH	bond-dissociation enthalpies
BxPC-3	human primary pancreatic adenocarcinoma
CoQ	coenzyme q10
δ	chemical shift in parts per million
J	coupling constant (in nmr spectrometry)
DPPH	2,2-diphenyl-1-picrylhydrazyl radical
FRAP	ferric ion reducing antioxidant power
HBA	number of hydrogen bond acceptor
HBD	number of hydrogen bond donor
HAT	hydrogen atom transfer
hTERT-HPNE	normal pancreas cell line

Electronic supplementary material The online version of this article (doi:10.1007/s00044-016-1660-5) contains supplementary material, which is available to authorized users.

✉ Azhar Ariffin
azhar70@um.edu.my

✉ Kok Hoong Leong
leongkh@um.edu.my

[1] Department of Chemistry, Faculty of Science, University of Malaya, 50603 Kuala Lumpur, Malaysia

[2] Department of Medical Analysis, College of Health and Medical Technologies, P.O. 10047, Baghdad, Iraq

[3] Department of Biomedical Science, Faculty of Medicine, University of Malaya, 50603 Kuala Lumpur, Malaysia

[4] Integrative Pharmacogenomics Institute (iPROMISE) Level 7, FF3 Building, Universiti Teknologi MARA, 42300 Bandar Puncak Alam, Selangor, Malaysia

[5] Department of Pharmacy, Faculty of Medicine, University of Malaya, 50603 Kuala Lumpur, Malaysia

[6] Center for Natural Product and Drug Discovery (CENAR), Department of Chemistry, Faculty of Science, University of Malaya, 50603 Kuala Lumpur, Malaysia

IC_{50}	half-maximum inhibitory concentration
log p	logarithm of partition coefficient
MCF-7	human breast adenocarcinoma cells
MDA-MB-231	human breast adenocarcinoma
MTT assay	cell proliferation colorimetric assay

Introduction

Reactive oxygen species (ROS), known as mediators of intracellular signaling cascades, are chemically reactive molecules containing oxygen (Kotaiah et al., 2012). Most living organisms can produce ROS and metabolize excessive amounts through normal physiological processes. Accumulation of excessive ROS is generally responsible for damaging lipids, proteins, and the DNA of cells, leading to oxidative stress (Nordberg and Arnér, 2001). As scientific research unravels the root cause of cancer, evidence of oxidative stress leading to chronic inflammation of cells is believed to perpetuate this genetic instability (Kundu and Surh, 2012). In particular, chronic excessive ROS is one of the underlying reasons for the development of cancer (Wu et al., 2014). Cancer is still a global health concern, with 12.7 million new cases reported in 2008, and is projected to reach 22.2 million cases by 2030 (Vineis and Wild, 2014). Genetic instability is recognized as a hallmark of cancer development, resulting in abnormal cell growth. In cases where a cancerous tumor has metastasized, the survival rate is drastically reduced (Ferrari et al., 2010). In an effort to reduce the damaging effects of ROS, antioxidants capable of scavenging excess ROS have received much attention in cancer therapy (Fuchs-Tarlovsky, 2013). Phenolic compounds represent an important class of antioxidants (Tung et al., 2007). Some examples, such as curcumin, resveratrol, and epigallocatechin, possessing both antioxidant and anticancer properties, have received great scientific interest. Additionally, these compounds suppress the proliferation of cancer cells and induce cell apoptosis. Apoptosis is a mechanism of programmed cell death that occurs naturally when cells are beyond repair or has abnormalities (Prasad et al., 2014; Tang et al., 2011). Recent research indicates that the inhibitory effects of phenolic antioxidant compounds stem mainly from their free radical scavenging properties, and a large amount of evidence supports their chemoprotective effects against oxidative stress-mediated disorders (Soobrattee et al., 2005). The inhibitory effects of phenols are further demonstrated by the observation that the presence of sulphur compounds classified as secondary antioxidants, e.g., sulphides, can decompose peroxides that are intermediates in the oxidation reactions and regenerate the primary antioxidants (Pospíšil, 1993).

The 1,3,4-oxadiazoles are an important class of heterocyclic bioactive compounds (Omar et al., 1996). Their widespread use as scaffolds in medicinal chemistry establishes this moiety as a member of the class of privileged structures. Differently substituted 1,3,4-oxadiazoles have been found to exhibit anti-inflammatory,analgesic, anticancer, antioxidant, and antifungal activities (Rapolu et al., 2013; Husain et al., 2009; Desai et al., 2013; Revanasiddappa and Subrahmanyam, 2009; Zhang et al., 2013). Additionally, Schiff base-containing compounds have been widely investigated and have received significant attention in chemistry and biology due to their anti-inflammatory, antioxidant, and anticancer activities (Hegazy and Ali, 2012; Alam et al., 2012; Ren et al., 2002; T'ang et al., 1985).

Employing the early evaluation of drug-likeness in the discovery and design process has assisted medicinal chemists in selecting leads with satisfactory biopharmaceutical properties (Bergström et al., 2013). Lipinski's Rule of Five (ROF) is a simple and widespread strategy employed in selecting leads. Developed by Chris Lipinski and his colleagues at Pfizer, the ROF is based on four influential properties identified from Pfizer's library of compounds, namely, molecular weight (MW), clog P, number of hydrogen bond donors (HBD) and number of hydrogen bond acceptors (HBA). The authors noted that compounds with poor absorption or permeability violate the boundaries of more than one of the four properties, which are a MW >500, Clog P >5, number of HBD exceeding 5 and HBA exceeding 10 (Lipinski et al., 1997, 2001). However, oral bioavailability does not solely rely on passive permeability as observed in the ROF. It involves a complex interplay of factors, such as active transporters and first-pass metabolizing enzymes. This complexity explains the observation that not all FDA-approved drugs meet the ROF; in fact, approximately 30 % of the drugs violate the ROF (Zhang and Wilkinson, 2007). Veber and colleagues from GlaxoSmithKline improved upon the ROF with the addition of molecular rigidity (measured by the number of rotatable bonds (NROTB)) and molecule accessibility (measured by the polar surface area (PSA)) based on oral bioavailability in rats. Compounds with 10 or fewer NRTOB and PSAs equal to or less than 140 $Å^2$ are assumed to have acceptable oral bioavailability (Veber et al., 2002). At the dawn of twenty-first century, the availability of human intestinal absorption data coupled with advancements in computational processing power brought about the construction of predictive computer models to assist medicinal chemists. One of the earliest was developed by Egan and colleagues in 2002 and has been a useful tool in predicting human intestinal absorption. The model predicts whether a compound lies within the regions of 95 % or 99 % confidence ellipses of well-absorbed compounds (Egan and Lauri, 2002).

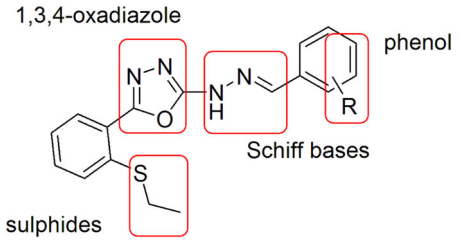

Fig. 1 Phenols, sulphides, 1,3,4-oxadiazoles and Schiff bases in a compact structure to incorporate active pharmacophore features for antioxidant and cytotoxic activities

With the previously mentioned hypothesis in mind, we aimed to combine the beneficial effects of phenols, sulphides, 1,3,4-oxadiazoles and Schiff bases in a compact structure with expected antioxidant and cytotoxic activities by synthesizing new 1,3,4-oxadiazole derivatives with the core structure shown in (Fig.1). Furthermore, a computational study predicting the absorption properties of the synthesized compounds was performed using the Lipinski rule, the Veber rule, and Egan's model.

Materials and methods

Chemicals

All chemicals and solvents were of analytical grade and purchased from Sigma-Aldrich (St. Louis, MO, USA) and Merck (Frankfurter StraBe, Darmstadt, Germany). Thin layer chromatography was performed on pre-coated silica gel plates (Si, 60, F254) for monitoring reactions and determining purity. Melting points were determined using a MEL-TEMP II apparatus and are uncorrected. IR spectra were recorded from 4000–400 cm^{-1} using a Perkin Elmer 400 Fourier transform infrared spectrometer (Waltham, MA, USA). ^{1}H NMR and ^{13}C NMR spectra were recorded on a BRUKER-AVN III 400 MHz (Fallanden, Switzerland) instrument using DMSO-d_6 and $CDCl_3$ as solvents and TMS as an internal standard. Mass spectra were recorded on an Agilent 5975 (Santa Clara, CA, USA) for EI/MS and Finnegan TSQ 7000 for HREI/MS.

Synthesis

*5-[2-(ethylsulfanyl)phenyl]-2,3-dihydro-1,3,4-oxadiazole-2-thione (**1**)*

White powder (EtOH), this compound was prepared as follows: potassium hydroxide (0.21 g, 3.75 mmol) was added to a solution of 2-(ethylsulphanyl) benzohydrazide (1 g, 3.75 mmol) and an excess of carbon disulphide (0.8 g, 0.6 mL) in absolute ethanol. The mixture was heated at reflux for 18 h, and the solvent was evaporated. Distilled water (25 mL) was added to the resulting residue, which was then filtered. Hydrochloric acid (5 %, 2 mL) was added and the filtered white precipitate was washed with water and recrystallized from ethanol to give the pure compound. It was obtained as a white solid powder (Yield: 84 %); m.p. 178–180 °C; IR. (KBr) ν_{max} 3314, 3219, 3059, 2959, 1602, 1558, 1337 cm^{-1};1H NMR (DMSO-d_6, 400 MHz): $\delta = 1.28$ (3H, t, $J = 7.02$ Hz, S–CH_2CH_3), 3.06 (2H, q, $J = 7.32$ Hz, S–CH_2), 7.35 (1H, ddd, $J = 7.9$ Hz, H6), 7.57 (2H, m, $J = 8.5$ Hz, H4, H5), 7.81 (1H, dd, $J = 8.4$ Hz, H7), 14.83 (1H, br s, NH);[13] CNMR (DMSO-d_6, 100 MHz): $\delta = 13.27$ (CH_3, S–CH_2CH_3), 25.67 (CH_2, S–CH_2), 119.93 (C, C6), 124.87 (C, C4),126.70 (C, C8), 129.51 (C, C7), 132.06 (C, C5), 138.18 (C, C3), 159.46 (C, C9, C=N), 176.99 (C, C10, C=S); HREIMS *m/z* (pos): 237.0155 $C_{10}H_9N_2OS_2$ (calcd. 237.0162).

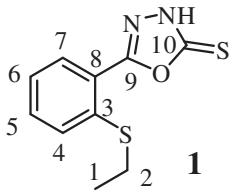

1

*Ethyl 2-({5-[2-(ethylsulfanyl)phenyl]-1,3,4-oxadiazol-2-yl} sulfanyl)-acetate (**2**)*

Yellowish solid (ethanol-ethyl acetate), this compound was synthesized when ethyl bromoacetate (1 g, 10 mmol) was added to a solution of compound **1** (2 g, 10 mmol) and anhydrous K_2CO_3 (1.3 g) in dry acetone. The mixture was stirred for 18 h at room temperature. The solvent was removed by evaporation and ethyl acetate (15 mL) was added. The mixture was left at room temperature to allow the product to precipitate. The solid product was filtered and recrystallized from ethanol-ethyl acetate (1:2). It was obtained as a pale yellow solid, (Yield: 78 %); m.p. 46 °C; IR. (KBr) ν_{max}2931, 2871, 1729, 1591 cm^{-1}.1H NMR ($CDCl_3$, 400 MHz): $\delta = 1.31$ (3H, t, $J = 7.2$ Hz, S–$CH_2\underline{CH_3}$), 1.39 (3H, t, $J = 6.9$ Hz, $OCH_2\underline{CH_3}$), 3.02 (2H, q, $J = 6.8$ Hz, S–$\underline{CH_2}$), 4.13 (2H, q, $J = 7.0$ Hz, $O\underline{CH_2}$), 4.16 (2H, s, $J = 6.9$ Hz, SCH_2), 7.26 (1H, m, J = 7.4 Hz, H6), 7.44 (2H, m, $J = 7.6$ Hz, H4, H5), 7.85 (1H, dd, $J = 8.4$ Hz, H7); 13C NMR ($CDCl_3$, 100 MHz): $\delta = 13.45$ (CH_3, S–CH_2CH_3), 14.08 (CH_3, C14, OCH_2CH3), 26.91 (CH_2, S–CH_2CH_3), 34.42 (CH_2, C11, S–CH_2), 62.39 (CH_2, C13, OCH_2), 121.64 (C, C6), 124.69 (C, C7), 126.93 (C, C4), 129.81 (C, C5), 131.38 (C, C8), 139.07 (C, C3), 162 (C, C9), 165.22 (C, C10), 167.45 (1C, C12); HREIMS *m/z* (pos): 325.0687 $C_{14}H_{17}N_2O_3S_2$ (calcd. 325.0675).

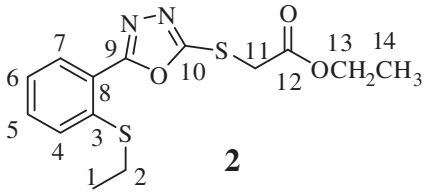

2

*2-[2-(Ethylsulfanyl)phenyl]-5-hydrazinyl-1,3,4-oxadiazole (**3**)*

White powder: this compound was synthesized from the addition of a solution of hydrazine hydrate (80 %, 2 mL) to compound **2** (2 g, 5 mmol) in dioxane (25 mL) and the mixture was allowed to stir for 48 h at room temperature). The solvent was evaporated under reduced pressure resulting in the formation of a pure white solid (Yield: 69 %); m.p. 86 °C; IR. (KBr) ν_{max} 3490, 3328, 3020, 3081, 2975, 1662, 1642 cm^{-1}.1H NMR (DMSO-d_6, 400 MHz): $\delta = 1.26$ (3H, t, $J = 7.3$ Hz, S–CH_2CH_3), 3.01 (2H, q, $J = 7.4$ Hz, S–CH_2), 4.51 (2H, br s, $J = 5.0$ Hz, NH_2), 7.3 (1H, m, $J = 7.9$ Hz, H6), 7.49 (2H, m, $J = 8.0$ Hz, H4, H5), 7.68 (1H, d, $J = 8.2$ Hz, H7), 8.62 (1H, s, NH); 13C NMR (DMSO-d_6, 100 MHz): $\delta = 13.21$ (CH_3, S–CH_2CH_3), 25.59 (CH_2, S–CH_2), 121.53 (C, C6), 124.78 (C, C7), 126.41 (C, C4), 128.93 (C, C5), 130.99 (C, C8), 137.25 (C, C3), 157.17 (C, C9) 165.72 (C, C10); HREIMS: *m/z* (pos): 236.0733 $C_{10}H_{12}N_4O_1S_1$ (calcd. 236.0732).

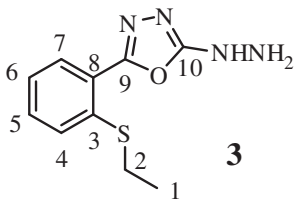

3

General procedure for the synthesis of compounds (4a–e)

The appropriately substituted hydroxybenzaldehyde (1 mmol) was added in small portions with stirring to a solution of Compound **3** (0.25 g, 1 mmol) in absolute ethanol (15 mL), and the mixture was heated at reflux for 6 h. The mixture was cooled and the precipitate that formed was washed and recrystallized from ethanol.

*4-[(1E)-(2-{5-[2-(ethylsulfanyl)phenyl]-1,3,4-oxadiazol-2-yl}hydrazin-1-ylidene)methyl]phenol (**4a**)*

Using 4-hydroxybenzaldehyde, colorless solid (Yield: 90 %); m.p. 198–200 °C; IR. (KBr) ν_{max} 3676 (OH phenol), 3322, 2981, 1633 cm^{-1};1H NMR (DMSO-d_6, 400 MHz): $\delta = 1.29$ (3H, t, $J = 7.3$ Hz, S–CH_2CH_3), 3.04 (2H, q, $J = 7.4$ Hz, SCH_2), 6.84 (2H, m, $J = 7.5$ Hz, H14), 7.34 (1H, m, $J = 7.4$ Hz, H6), 7.53 (4H, m, $J = 7.7$ Hz, H4, H5, H13), 7.79 (1H, d, $J = 8.5$ Hz, H7), 8.06 (1H, s, CH=N), 9.9 (1H, s, OH), 11.88 (1H, s, NH); 13C NMR (DMSO-d_6, 100 MHz): $\delta = 13.84$ (CH_3, S–CH_2CH_3), 26.19 (CH_2, S–CH_2), 116.15 (2C, C14), 122.37 (C, C6), 125.30 (C, C12), 125.62 (C, C7), 127.19 (C, C4), 128.82 (2C, C13) 129.50 (C, C5), 131.36 (C, C8), 138.04 (C, C3), 145.55 (C, C11), 157.89 (C, C15), 159.52 (C, C9), 161.94 (C, C10); HREIMS: *m/z* (pos): 340.0992 $C_{17}H_{16}N_4O_2S_1$ (calcd. 340.0994).

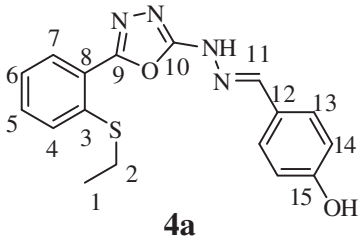

4a

*4-[(1E)-(2-{5-[2-(ethylsulfanyl)phenyl]-1,3,4-oxadiazol-2-yl}hydrazine-1-ylidene)methyl]-2-methoxyphenol (**4b**)*

Using 4-hydroxy-3-methoxy benzaldehyde, colorless solid (Yield: 85 %); m.p. 100–102 °C; IR. (KBr) ν_{max} 2951, 1631 cm^{-1}.1H NMR (DMSO-d_6, 400 MHz): $\delta = 1.28$ (3H, t, $J = 7.2$ Hz, S–CH_2CH_3), 3.04 (2H, q, $J = 7.3$ Hz, S–CH_2), 3.82 (3H, s, OCH_2CH_3), 6.83 (1H, d, $J = 7.2$ Hz, H14), 7.1 (1H, dd, $J = 7.1$ Hz, H6), 7.32 (2H, m, $J = 7.4$ Hz, H5, H13), 7.52 (2H, m, $J = 7.3$ Hz, H4, H17), 7.79 (1H, d, $J = 7.7$ Hz, H7) 8.05 (1H, s, CH=N), 9.51 (1H, s, OH), 11.89 (1H, s, NH); 13C NMR (DMSO-d_6, 100 MHz): $\delta = 18.58$ (CH_3, S–CH_2CH_3), 30.98 (CH_2, S–CH_2), 60.76 (CH_3, OCH_3), 114.36 (C, C17), 120.68 (C, C14), 126.44 (C, C13), 127.07 (C, C6), 130.14 (C, C7), 130.76 (C, C4) 132.01 (C, C12), 134.35 (C, C5), 136.27 (C, C8), 142.70 (C, C3), 150.79 (C, C11), 153.17 (C, C16), 153.72 (C, C15), 162.73 (C, C9), 166.65 (C, C10); HREIMS *m/z* (pos): 370.1086 $C_{18}H_{18}N_4O_3S_1$ (calcd. 370.1100).

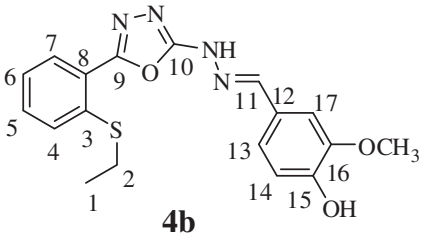

4b

*2-Ethoxy-4-[(1E)-(2-{5-[2-(ethylsulfanyl)phenyl]-1,3,4-oxadiazol-2-yl}hydrazine-1-ylidene)methyl]phenol (**4c**)*

Using 4-hydroxy-3-ethoxybenzaldehyde, colorless solid (Yield: 89 %); m.p. 204 °C; IR. (KBr) ν_{max} 3545, 2931,

1634 cm^{-1}. 1H NMR (DMSO-d_6, 400 MHz): $\delta = 1.28$ (3H, t, $J = 7.3$ Hz, S–CH_2CH_3), 1.36 (3H, t, $J = 7.0$ Hz, OCH_2CH_3), 3.04 (2H, q, $J = 7.3$ Hz, S–CH_2), 4.07 (2H, q, $J = 6.9$ Hz, OCH_2), 6.84 (1H, d, $J = 7.3$ Hz, H14), 7.09 (1H, dd, $J = 8.2$ Hz, H6), 7.25 (1H, d, $J = 1.8$ Hz, H5), 7.34 (1H, m, H13) 7.54 (2H, m, $J = 8.2$ Hz, H4, H17), 7.78 (1H, d, $J = 8.0$ Hz, H7) 8.04 (1H, s, CH=N), 9.42 (1H, s, OH), 11.88 (1H, s, NH). 13C NMR (DMSO-d_6, 100 MHz): $\delta =$ 13.29 (CH_3, S–CH_2CH_3), 14.47 (CH_3, OCH_2CH_3) 25.77 (CH_2, S–CH_2), 63.92 (CH_2, OCH_2), 110.27 (C, C17), 115.45 (C, C14), 121.33 (C, C13), 121.65 (C, C6), 124.97 (C, C7), 125.49 (C, C4) 126.80 (C, C12), 129.18 (C, C5), 131.21 (C, C8), 137.37 (C, C3), 145.93 (C, C11), 147.01 (C, C16), 148.57 (C, C15), 157.57 (C, C9), 161.40 (C, C10); HREIMS *m/z* (pos): 384.1257 [M+] (calc. for C19H20N4O3S1 384.1256).

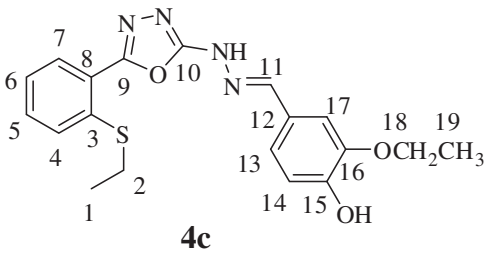

4c

*2,6-di-tert-butyl-4-[(1E)-(2-{5-[2-(ethylsulfanyl)phenyl)-1,3,4-oxadiazol-2-yl)-hydrazin-1-ylidene)methyl]phenol (**4d**)*

Using 3,5-di-tert-butyl-4-hydroxybenzaldehyde, colorless solid, (Yield: 90 %); m.p 216 °C; IR. (KBr) ν_{max} 3630, 3313, 3214, 2956, 1643 cm^{-1}.1H NMR (DMSO-d_6, 400 MHz): $\delta = 1.28$ (3H, t, $J = 7.3$ Hz, S–CH_2CH_3), 1.41 (18H, s, 2× *t*-Bu), 3.04 (2H, q, $J = 7.4$ Hz, CH_2), 7.35 (2H, m, phenolic OH and H4), 7.46 (2H, s, H13), 7.53 (2H, d, $J = 3.8$ Hz, H5, H6), 7.77 (1H, d, $J = 7.7$ Hz, H7) 8.08 (1H, s, CH=N), 11.86 (1H, s, NH).13C NMR (DMSO-d_6, 100 MHz): $\delta = 13.42$ (CH_3, S–CH_2CH_3), 25.77 (CH_2, S–CH_2), 30.11 (6C, 2× –C$(CH_3)_3$), 34.4 (2C, 2× –C$(CH_3)_3$, 122.04 (2C, C13), 123.38 (C, C12), 124.92 (C, C6), 125.47 (C, C7), 126.91 (C, C4), 129.05 (C, C5), 130.97 (C, C8), 137.34 (C, C14), 139.24 (C, C3), 146.04 (C, C=N, C11), 155.37 (C, C15), 157.53 (C, C=O, C9), 161.49 (C, C=N, C10); HREIMS *m/z* (pos): 452.2239 $C_{25}H_{32}N_4O_2S_1$ (calcd. 452.2246).

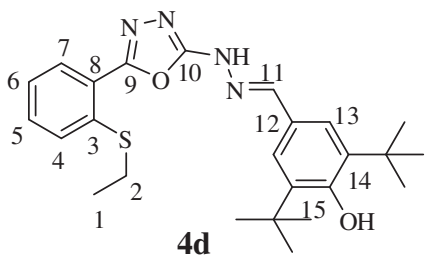

4d

*2-Bromo-4-chloro-6-[(1E)-(2-{5-[2-(ethylsulfanyl)phenyl]-1,3,4-oxadiazol-2-yl}-hydrazin-1-ylidene)methyl]phenol (**4e**)*

Using 3-bromo-5-chloro-2-hydroxybenzaldehyde, colorless solid (Yield: 88 %); m.p. 202–204 °C; IR. (KBr) ν_{max} 3545, 2949, 1632 cm^{-1}.1H NMR (DMSO-d_6, 400 MHz): $\delta = 1.3$ (3H, t, $J = 7.3$ Hz, CH_3), 3.06 (2H, q, $J = 7.4$ Hz, CH_2), 7.36 (1H, ddd, $J = 7.9$, H15), 7.55 (2H, m, H5, H6), 7.69 (2H, dd, $J = 9.2$ Hz, H4, H13), 7.8 (1H, m, H7), 8.34 (1H, br.s, CH=N), 11.46 (1H, br.s, OH), 12.69 (1H, s, NH); 13C NMR (DMSO-d_6, 100 MHz): $\delta = 13.32$ (CH_3, S–CH_2CH_3), 25.75 (CH_2, SCH_2), 111.02 (C, C16), 121.19 (C, C12), 121.52 (C, C6), 123.62 (C, C7), 124.87 (C, C4), 126.80 (C, C14) 128.22 (C, C13), 129.10 (C, C5), 131.22 (C, C8), 132.52 (C, C15), 137.71 (C, C3), 144.09 (C, C11), 152.36 (C, C17), 158.01 (C, C9), 160.56 (C, C10); HREIMS *m/z* (pos): 451.9707 $C_{17}H_{14}N_4BrClO_2S_1$ (calcd. 451.9709).

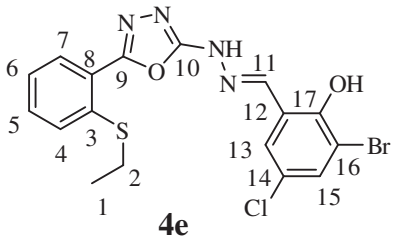

4e

In silico drug-likeness evaluation

Discovery Studio 4.0 software (Accelrys Incorporation, San Diego, CA, USA) was used to calculate the MW, calculated log P (clog P), number of HBA and HBD for the Lipinski rule; NROTB and PSA for the Veber rule; and, predicting the human intestinal absorption based on Egan's model, which were available in the ADMET module of the software.

Antioxidant activities

DPPH radical scavenging assay

DPPH assay is one of the tests used to prove the ability of the compounds to act as donors of hydrogen atoms. As the DPPH free radical molecule has a single electron, it gives rise to a deep violet color, characterized by an absorption band in methanol solution at about 515 nm. When a solution of DPPH is mixed with an antioxidant compound that can donate a hydrogen atom, this gives rise to the reduced form of DPPH (non radical DPPH) with the loss of its deep violet color (Prior et al., 2005). The scavenging activity of stable 2,2 Diphenyl-1-picryl dyhydrazyl free radical was determined according to the method of (Gerhäuser et al., 2003),

with slight modifications. (1 mg/1 mL) of the synthesized compound and the reference standards were prepared as stock solutions then a series of dilution solutions with five varying concentrations were tested. 5 µL of samples/standards were loaded, and followed by 195 µL of DPPH reagent, the mixtures were then mixed vigorously and incubated in the dark at room temperature for 2 h, and the absorbance was measured spectrophotometrically at 515 nm at intervals of 20 min for 3 h. The percentage of DPPH free radical scavenging activity was calculated as: DPPH (%) = [(Abs of blank−Abs of sample)/absorbance of sample] × 100. The results were expressed as (half-maximum inhibitory concentration (IC_{50}) value) the compounds concentration that required to reduce 50 % of the hydroxyl radical produced.

Ferric ion reducing antioxidant power (FRAP) assay

The reducing capacities of the synthesized compounds were measured by the method of Benzie and Strain (Benzie and Strain, 1996), with modifications. A total of 10 mL of 300 mM acetate buffer was adjusted to pH 3.6 by mixing with 3.1 g $CH_3COONa{\cdot}3H_2O$ and 16 mL of glacial acetic acid. The TPTZ (2,4,6-tripyridyl-*s*-triazine) solution was prepared by dissolving 10 mM TPTZ in 40 mM HCl. Then, 1 mL of the TPTZ solution was mixed with the ferric ion reducing antioxidant power (FRAP) solution and 1 mL of 20 mM ferric chloride hexahydrate in distilled water. The FRAP solution was warmed to 37 °C, and the synthesized compounds were added and allowed to react in the dark. Absorbance was monitored spectrophotometrically at 593 nm. After that 10 µL of compound or standard and 90 µL of distilled water were added to 300 µL of the working FRAP reagent. Absorbance was measured (593 nm) at 0 min immediately upon addition of the working FRAP reagent after vortexing. Thereafter, absorbance reading was taken after 4 min. All results were expressed as µM ferrous per g dry mass and were compared with that of reference compounds. The results are expressed as mean ± standard deviation of triplicates.

Cytotoxic screening

Cell culture

Human cancer and normal cell lines were obtained from American Type Culture Collection (ATCC) (Manassas, VA, USA). Dulbecco's modified Eagle's medium (DMEM), Hanks' Balanced Salt Solution (HBSS), 100 mM non-essential amino acids, phosphate buffer solution (pH 7.2), gentamycin and amphotericin B were purchased from Invitrogen Corporation (Carlsbad, CA, USA). L-glutamine, fetal bovine serum (FBS), 0.25 % trypsin-EDTA, dimethyl sulphoxide (DMSO), curcumin, vinblastinesulfate and 4,5-dimethylthiazol-2-yl-2,5-diphenyltetrazoliumbromide (MTT) were purchased from Sigma-Aldrich (St. Louis, MO, USA).

Cytotoxicity assay

The cytotoxicity of the compounds was evaluated against three types of cancer cell lines, namely, pancreatic (BxPC-3), non-metastatic (MCF-7) and metastatic breast (MDA-MB-231), as well as a normal pancreatic cell line (hTERT-HPNE). Cell lines were cultured in DMEM media supplemented with 2 mM L-glutamine, 10 % FBS, 50 µg/mL gentamycin and 2.5 µg/mL amphotericin B, and maintained in a 37 °C humidified atmosphere of 5 % CO_2 in a cell incubator. Compounds **1–4e** and the positive control (curcumin and vinblastine sulfate) were dissolved in DMSOand further diluted with DMEM media to yield a final DMSO concentration of <0.5 % (v/v). Cells were plated into 96-well microplates at a density of 10^4 cells per well and maintained in a cell incubator for 24 h. Then 100 µL of samples were introduced in triplicate to give a final concentration range of 100–1.56 µM. For the negative control,cells were treated with vehicle (0.5 % v/v DMSO) only. Cells were further incubated for 72 h, and then, cell viability was determined. Culture media were carefully refreshed with 100 µL of HBSS, followed by 50 µL per well of MTT reagent (2 mg/mL). Microplates were returned to the incubator for 2 h, after which the supernatant was removed and the formazan crystals were dissolved in 100 µL of DMSO. The absorbance of the formazan product was read on a microplate reader at 570 nm, with 620 nm as the background wavelength (Infinite 200, Tecan, Männedorf, Switzerland). The IC_{50}'s of the samples and the positive control were determined from dose-response curves using Prism 5.02 software (GraphPad Software Inc., La Jolla, CA, USA) (Looi et al., 2013). The results are expressed as mean ± standard deviation of triplicates.

Apoptosis and cell cycle analysis

Apoptosis and cell cycle analysis were performed separately using commercial Annexin V: FITC Apoptosis Detection Kit I and CycleTest™ Plus DNA Reagent kit, respectively (BD Bioscience, NJ, USA). Cells were seeded at a density of 5×10^5 cells per well in six-well plates. After overnight attachment, cells were treated with compound at 13, 26 and 52 µM for 72 h in apoptosis analysis and 13 µM for 24, 48 and 72 h in cell cycle analysis. After treatment, cells were harvested, centrifuged at 1500 × g for 5 min and cell staining was performed according to the manufacturer's instructions. DNA QC Particles kit was used to calibrate the

FACSCanto II flowcytometer (BD Biosciences, NJ, USA). Cell populations were subjected to cytometry analysis and the quadrants were set according to the population of viable cells in untreated samples. Three independent experiments were performed and in each experiment, a total of 10,000 events were collected for both apoptosis and cell cycle analysis. FacsDiva 5.0.3 software was used to calculate the percent of cells in the respective quadrants for apoptosis analysis and Mod Fit LT software (Verity Software House Inc., Topsham, ME, USA) for cell cycle analysis (Looi et al., 2013). The results are expressed as mean ± standard deviation and statistical significant were calculated using Prism 5.02 software's paired Student's *t*-test against controls (GraphPad Software Inc., La Jolla, CA, USA).

Results and discussion

Chemistry

The 2-[2-substituted-hydrazinyl]-5-[2-(ethylsulphanyl)phenyl]-1,3,4-oxadiazole derivatives **4a–e** were synthesized according to the reaction sequence outlined in Scheme 1. 5-[2-(Ethylsulphanyl)phenyl]-1,3,4-oxadiazole-2(3H)-thione (**1**) was prepared by reaction of 2-(ethylsulphanyl)benzohydrazide with CS_2 in KOH. Treatment of (**1**) with ethyl bromoacetate gave the ethyl acetate analog (**2**) in good yield. Reaction of the ethyl acetate (**2**) with 80 % $N_2H_4{\cdot}H_2O$ yielded the proposed acid hydrazide (**3**), which was further reacted with differently substituted hydroxybenzaldehydes in the presence of ethanol to afford compounds **4a–e**. The structures of the synthesized compounds were confirmed by IR, ^{1}H NMR, and ^{13}C NMR spectroscopy and mass spectrometry.

In silico drug-likeness evaluation

Performing early evaluations of drug-likeness would be advantageous in filtering compounds with predicted poor biopharmaceutical properties. Drug-likeness encompasses the evaluation of structural or physical properties of a compound that is consistent with established drugs (Yehye et al., 2012). The drug-likeness of parent **1** and intermediates **2** and **3**, and derivatives **4a–4e** were evaluated based on the Lipinski rule. None of the compounds violated any of the rules, with the exception of compounds **4d** and **4e**, which violated only the clog P rule, where their values were >5 (Table 1). According to the Lipinski rule, violation of one parameter is still acceptable (Lipinski et al., 2001). However, it should be mentioned that approximately 30 % of FDA-approved drugs violate the Lipinski rule, and this is attributed to the inherent rigidity of the strict boundaries set by the rule (Zhang and Wilkinson, 2007; Petit et al., 2012).

On the other hand, based on the Veber rule, all of the compounds are within the rule's boundaries (Table 1). The differences in the Veber rule are the addition of molecular rigidity (NROTB) and molecule accessibility (PSA), developed after data mining the results of oral bio availabilities, in rats, of 1100 drug candidates (Veber et al., 2002). However, both the Lipinski and Veber rules share a common weakness in considering drug absorption as a univariate relationship. Therefore, it does not take into account interactions between the molecular properties or the multivariate relationships for the prediction of drug absorption (Egan and Lauri, 2002). Egan and colleagues

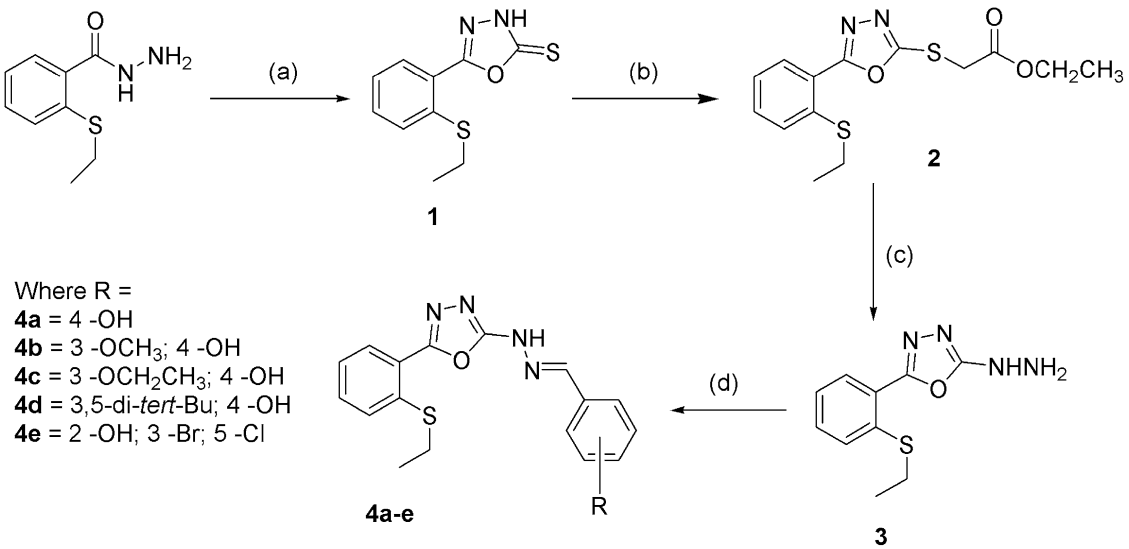

Scheme 1 Reaction scheme for the formation of compounds **4a–e.** Reagents and conditions: **a** (i) CS_2/KOH, EtOH, reflux 18 h; (ii) HCl; **b** ethyl bromoacetate, K_2CO_3, acetone, r.t., 18 h; **c** $NH_2NH_2.H_2O$, dioxane, r.t., 18 h; **d** ArCHO, EtOH, reflux 6 h

Table 1 Calculated molecular properties based on the Lipinski and Veber rules

Compounds	Based on Lipinski rule					Based on Veber rule	
	Violation of Lipinski rule (≤1)	HBA (≤10)	HBD (≤5)	clog P (≤5)	MW (≤500)	NROTB (≤10)	PSA (≤140 Å^2)
1	0	3	1	3.20	238.329	3	33.06
2	0	5	0	3.28	324.418	8	61.31
3	0	5	2	1.69	236.293	4	74.43
4a	0	6	2	3.97	340.400	6	80.03
4b	0	7	2	3.84	370.426	7	88.96
4c	0	7	2	4.18	384.452	8	88.96
4d	1	6	2	7.38	452.612	8	80.03
4e	1	6	2	5.36	453.741	6	80.03
Curcumin	1	6	3	2.17	368.380	7	97.61

HBA hydrogen bond acceptors, *HBD* hydrogen bond donors, *clog P* calculated logP, *MW* Molecular Weight, *NROTB* number of rotatable bonds, *PSA* polar surface area

built a computational model looking at multivariate factors that influence drug absorption. When they plotted the descriptors atom-based log P (AlogP) vs. PSA, they were able to cluster compounds within 95 % or 99 % confidence ellipses. They further explained that both lipophilicity (measured by Alog P) and hydrogen bonding ability (measured by PSA) are nonlinearly related to permeability. This enables the construction of a clustering model (ellipses) more useful than a quantitative model (Egan et al., 2000). When we assessed our compounds using Egan's model, compounds **1–4a–c** were within the 95 % confidence ellipse and compound **4e** was within the 99 % confidence ellipse for good absorption, whereas compound **4d** was predicted to have poor absorption (Fig. 2). It was noted that compound **4d** has a high log P value (7.38) (Table 1). A published report explained that a highly lipophilic compound will be highly partitioned in the lipid portion of a membrane and fail to pass through the aqueous portion of the membrane, which leads to its poor permeation across the intestinal barrier (Wils et al., 1994).

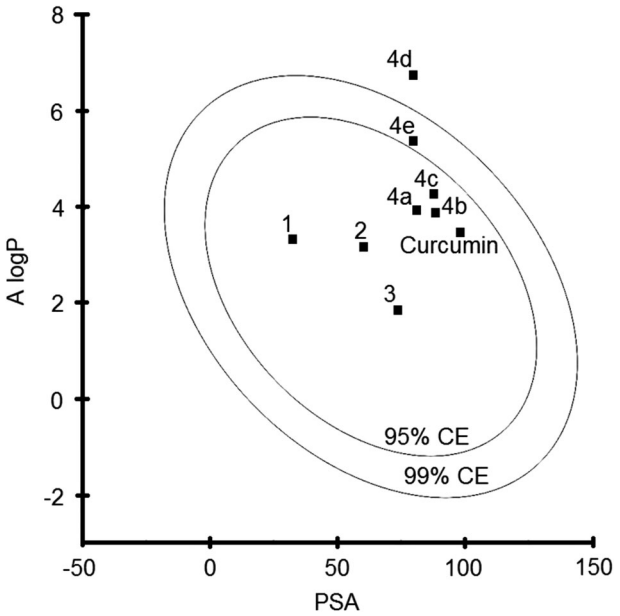

Fig. 2 Plot of AlogP versus PSA for compounds **1–4e** and curcumin based on Egan's model. *AlogP* atom-based log P,*PSA* polar surface area, *CE* confidence ellipse

Antioxidant activities

All of the newly synthesized compounds were evaluated for their free radical scavenging ability and compared with five positive controls—quercetin, BHT, trolox, rutin, and ascorbic acid, and the results are shown in Table 2. Compounds **1** and **3** showed the highest radical scavenging activities. Compounds **4a**, **4b**, **4d**, and **4e** demonstrated greater radical scavenging activities than BHT, trolox, rutin, and ascorbic acid. Compound **4c** exhibited lower IC_{50} than that of BHT but higher than those of the other tested compounds. Compound 2 was the only compound that did not show any radical scavenging activity in this assay.

The assay for reduction of iron (III) to iron (II) at low pH was performed to determine the FRAP values (μM/100 g) of the synthesized compounds in comparison with the positive controls. The results are shown in (Table 2). Compounds **3**, **4b**, **4c**, and **4d** displayed excellent FRAP values compared to the reference compounds. Compounds **2** and **4a** possessed greater FRAP reducing power than BHT, while compounds **1** and **4e** showed very poor FRAP values when compared to the reference compounds.

In the search for more potent leads through the incorporation of different pharmacophores into one structure, it is important to determine the structure–activity relationship of

the resulting compounds. In this study, two different in vitro antioxidant assays were carried out to evaluate the biological activities of the newly synthesized compounds – the DPPH radical scavenging assay and the FRAP assay. The total antioxidant capacity value should include methods applicable to both lipophilic and hydrophilic antioxidants with regards to the similarities and differences of both hydrogen atom transfer (HAT) and electron transfer (ET) mechanisms (Karadag et al., 2009). The DPPH assay involves both HAT and ET mechanisms, whereas the FRAP assay involves only the ET mechanism (Prior et al., 2005).

Table 2 DPPH scavenging activity (EC_{50} μg/mL), and FRAP values (μM/g) for the synthesized compounds (**1**, **2**, **3**, **4a**, **4b**, **4c**, **4d**, and **4e**)

Compounds	Scavenging activity DPPH[a] (IC_{50}[b] μg/mL)	FRAP[a] values (μM/g)
1	2.22 ± 0.01	43.83 ± 0.02
2	No activity	230.44 ± 0.14
3	2.21 ± 0.08	2561.11 ± 0.03
4a	3.96 ± 0.11	428.33 ± 0.09
4b	2.55 ± 0.01	2985.56 ± 0.09
4c	9.48 ± 0.05	1497.22 ± 0.04
4d	3.49 ± 0.12	1228.89 ± 0.03
4e	3.19 ± 0.08	46.83 ± 0.03
Quercetin	2.54 ± 0.07	1371.11 ± 0.26
BHT	18.71 ± 0.01	77.83 ± 0.08
Trolox	5.35 ± 0.64	987.78 ± 0.14
Rutin	5.25 ± 0.01	393.89 ± 0.02
Ascorbic acid	7.52 ± 0.08	1206.67 ± 0.02

[a]Each value represents the mean ± standard deviation of triplicates

[b]IC_{50}: 50 % effective concentration

HAT-based methods measure the classical ability of an antioxidant to scavenge free radicals by donating hydrogen to form stable compounds. ET-based methods detect the ability of a potential antioxidant to transfer one electron and reduce any compound, including metals, carbonyls, and radicals (Karadag et al., 2009).

Based on the results observed, we believe that the HAT mechanism is involved in the antioxidant activity. Compounds **1**, **3**, and **4a–e** contain an NH group that could easily transfer a H atom onto the DPPH radical thus demonstrated good radical scavenging activity. Compound **2** does not possess a NH or OH group and therefore, it could not transfer a H atom onto the DPPH radical, leading to its poor activity as an antioxidant.

In the case of compound **1**, the mechanisms of antioxidants are shown in Scheme 2. Assuming that the bond-dissociation energy of N–H is low, the scavenging of DPPH• by **1** is proposed in Scheme 2, in which hydrogen radicals are extracted from the N–H of the oxadiazole ring. This mechanism showed that compound **1** is able to suppress two DPPH• radicals.

The result shown in Table 2 indicates that the substituents on the benzene ring of the Schiff bases have little influence on the radical scavenging ability (except for compound **4c**). The IC_{50} value of compounds **4a**, **4b**, **4d** and **4e** does not differ very much with each other. Compound **4c** demonstrated the lowest radical scavenging activity. We could not offer any explanation at the moment as to why **4c**, which is very similar in structure with **4b**, but show poor radical scavenging activity.

For the monophenolic compounds **4a–e**, we proposed a different mechanism. Compound **4b** demonstrated the highest radical scavenging activity. The proposed

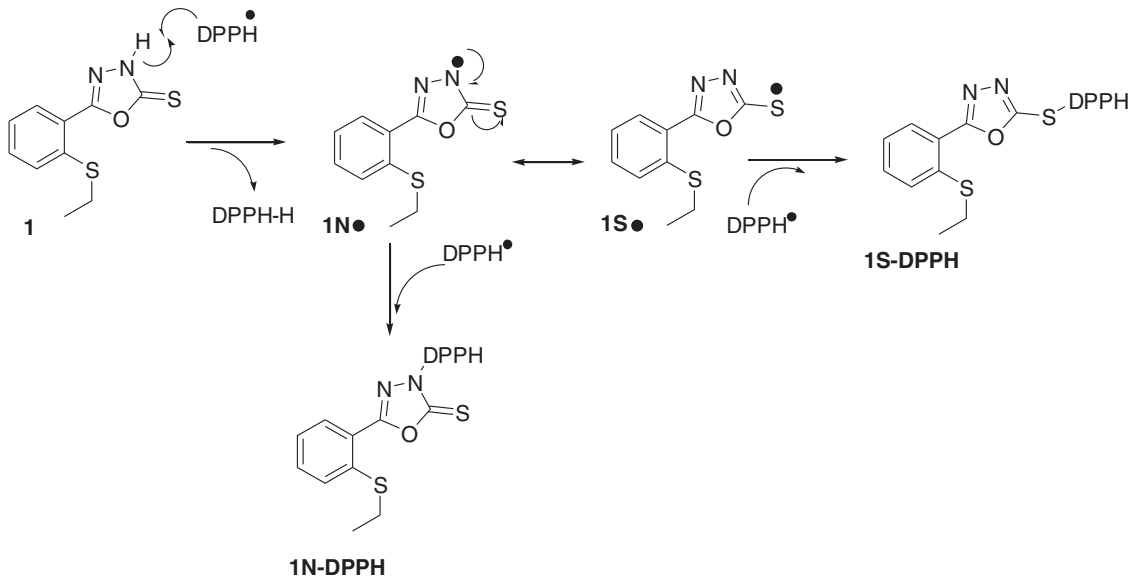

Scheme 2 Proposed HAT mechanism between compound **1** and the DPPH radical

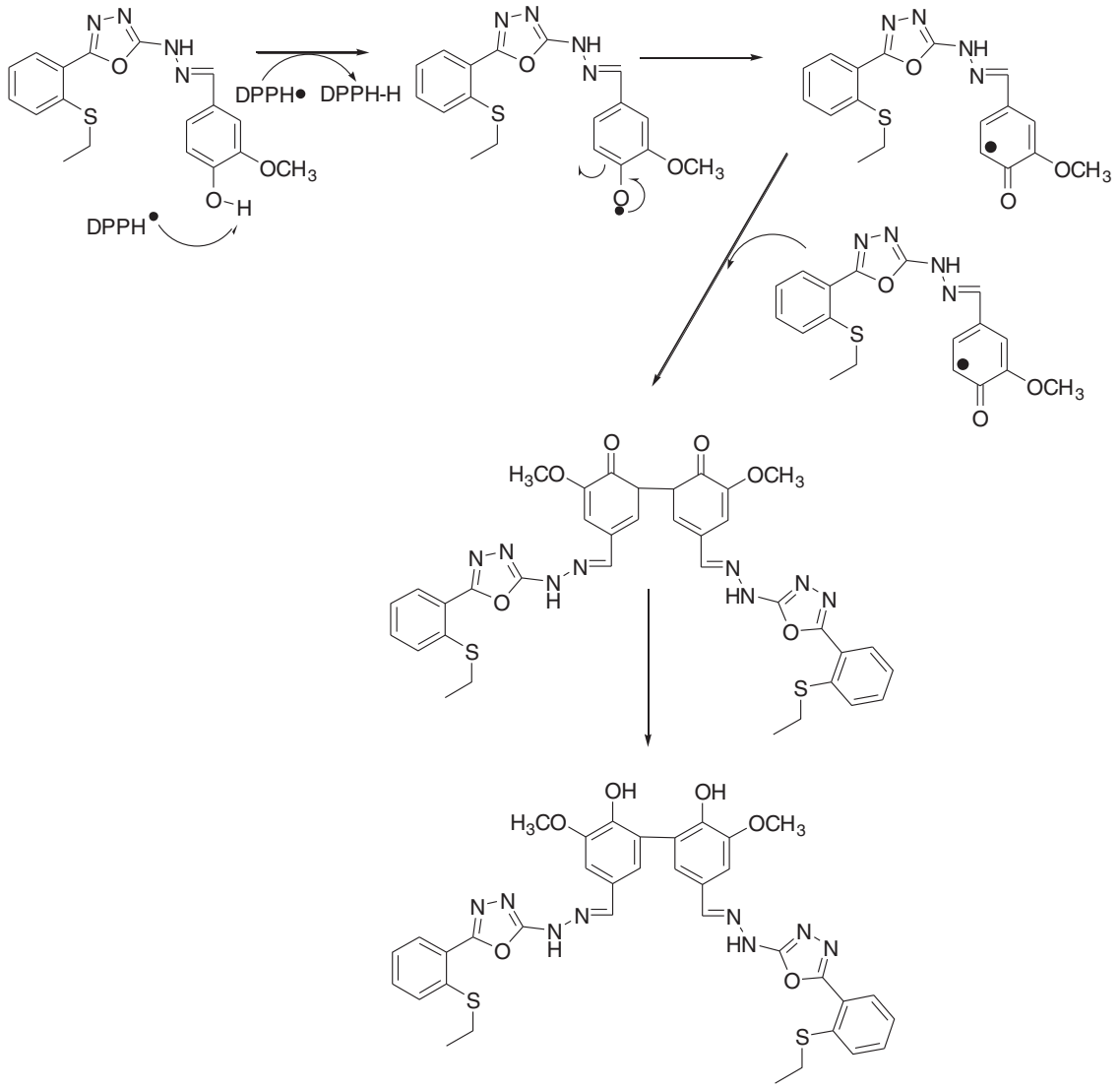

Scheme 3 Proposed HAT mechanism between compound **4b** and the DPPH radical

mechanism involves the dimerization between the resulting radicals as shown in Scheme 3. Brand-Williams has proposed a similar mechanism for phenoxy compounds with free *ortho-* and *para-* positions (Brand-Williams et al., 1995). After dimerization the two hydroxyl groups would be regenerated intramolecularly and could again interact with the DPPH radical.

From the FRAP assay data, comparison between compounds **4a–e** show that the presence of an electron donating group on the phenolic ring increases the reducing power of the compounds. On the other hand, the presence of electron withdrawing groups reduces the reducing power of the compounds. Compounds **4b** and **4c** contain strong electron donating ability through resonance by OMe and OEt group, respectively and therefore have strong reducing power compared to **4a**, which does not possess a substituent, as well as **4d**, which possesses a weak electron donating group. In contrast, compound **4e**, containing two strong electron withdrawing groups (Br and Cl), shows very poor reducing power.

Cytotoxic activity

The cytotoxic effects of the derivatives were investigated in vitro against the BxPC-3, MCF-7, and MDA-MB-231 cancer cell lines and the hTERT-HPNE normal cell line using the MTT assay. This colorimetric assay measures the percent of viable cells after exposure to a test compound (Malich et al., 1997). A dose-response curve is observed from cytotoxic compounds where the percentage of viable cells decreases with increasing concentrations of the compounds. The 50 % inhibitory concentration (IC_{50}) is obtained from the dose-response curve at the concentration where 50 % of the cells remain viable (Table 3). Positive

Table 3 IC_{50} values of compounds **1–4a–e** and curcumin obtained from their respective dose-response curves after 72 h treatment

Compounds	IC_{50} [a]μM			
	BxPC-3	hTERT-HPNE	MCF-7	MDA-MB-231
1	> 100	> 100	> 100	> 100
2	> 100	> 100	> 100	> 100
3	> 100	> 100	> 100	67.79 ± 9.22
4a	46.68 ± 1.38	60.45 ± 3.49	46.76 ± 1.01	63.07 ± 1.05
4b	43.85 ± 3.10	75.59 ± 0.26	53.90 ± 1.07	> 100
4c	26.17 ± 1.10	39.04 ± 3.01	36.49 ± 0.60	80.24 ± 1.50
4d	>100	>100	>100	>100
4e	31.07 ± 2.76	1.88 ± 0.29	39.54 ± 2.23	21.40 ± 1.22
Curcumin	47.85 ± 0.17	39.22 ± 0.25	61.20 ± 0.53	34.82 ± 1.36
Vinblastine sulfate	33.04 ± 2.14	22.81 ± 1.00	21.00 ± 2.33	27.06 ± 6.05

BxPC-3 pancreatic cancer cell line, *hTERT-HPNE* normal pancreatic cell line, *MCF-7* non-metastatic breast cancer cell line, *MDA-MB-231* metastatic breast cancer cell line. *IC_{50}* 50 % inhibition concentration

[a]Results are expressed as mean ± standard deviation of triplicates

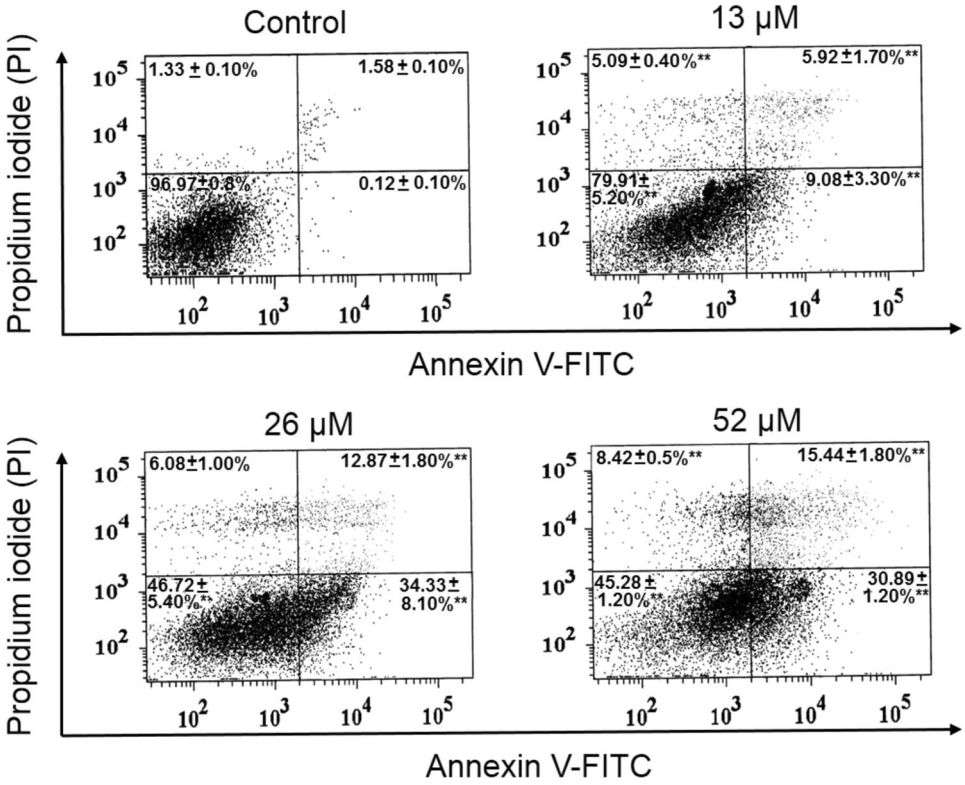

Fig. 3 Effects of compound **4c** on cell apoptosis of BxPC-3cells. Apoptosis was detected by AnnexinV-FITC/PI dual-staining after treatment with compound **4c** (13, 26, and 52 μM) for 72 h and 10,000 events were analyzed by flow cytometer. Results are expressed as mean ± standard deviation of three independent experiments, significant difference in comparison to controls is indicated as $^{**}p < 0.01$

controls, curcumin and vinblastine sulfate were used for comparison. Curcumin was selected because it contains two benzene rings that are substituted with –OH and –OMe groups, which has structural resemblance to our compounds (**4a–e**). Furthermore, curcumin has been reported to show anticancer and antioxidant potencies, which are related to the activities we are investigating in this study (Prasad et al., 2014). On the other hand, vinblastine sulfate is an anticancer drug clinically being used for the treatment of cancers. The derivatives revealed a moderate inhibitory effect against the cancer cell lines, comparable to curcumin and vinblastine sulfate. The monophenolic derivatives (**4a**, **4b**, **4c**, and **4e)** gave an inhibitory effect against the cancer cell lines, with the most potent being compound **4e** against MDA-MB-231 ($IC_{50} = 21.40 \pm 1.22$ μM) and **4c** against BxPC-3 ($IC_{50} = 26.17 \pm 1.10$ μM). However, the halogenated compound **4e** showed higher cytotoxicity against normal pancreatic cells (hTERT-HPNE $IC_{50} = 1.88 \pm 0.29$ μM) than pancreatic cancer cells (BxPC-3 $IC_{50} = 31.07 \pm 2.76$ μM). Compounds **1**, **2**, and **4d** exhibit low cytotoxic

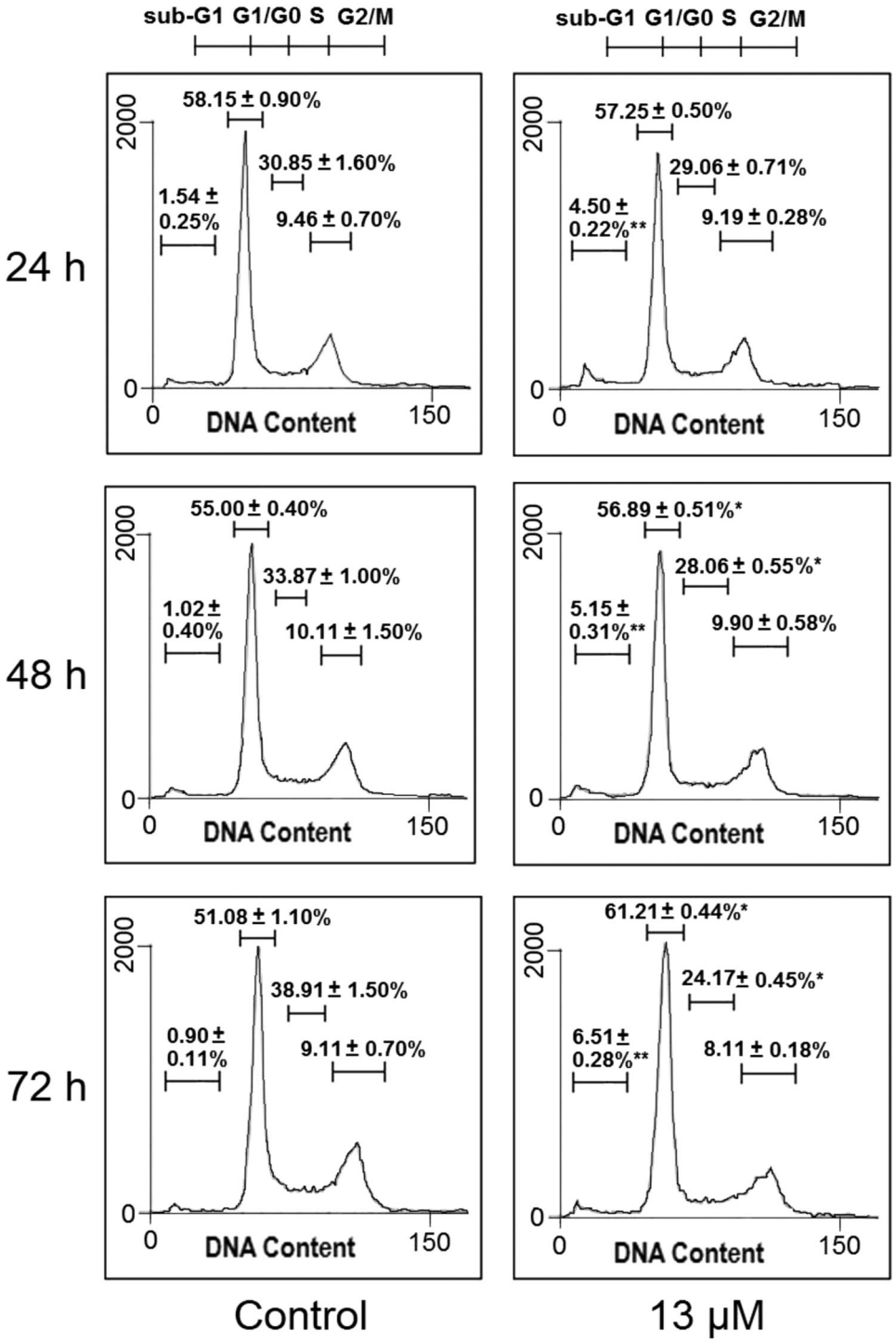

Fig. 4 Effects of compound **4c** on cell cycle of BxPC-3cells. Cells were with treated with compound **4c** (13 μM) for 24, 48, and 72 h, and the DNA content of 10,000 events was analyzed by flow cytometer. Results are expressed as mean ± standard deviation of three independent experiments, significant difference in comparison to controls are indicated as $*p < 0.05$ and $**p < 0.01$

activity against the cell lines tested, as their IC_{50} values were greater than 100 μM.

Apoptosis and cell cycle analysis

The poor survival rate of cancer patients in the early stages of chemotherapy could be attributed to the loss of potency when the cancer progresses into the metastatic stage, as well as non-specificity, which can cause serious side effects on normal healthy cells (Hoelder et al., 2012). Bearing this in mind, in addition to non-metastatic cancer cell lines (BxPC-3 and MCF-7), we employed normal cell lines (hTERT-HPNE) and metastatic cancer cell lines (MDA-MB-231) in our approach to evaluate the specificity and potency of the

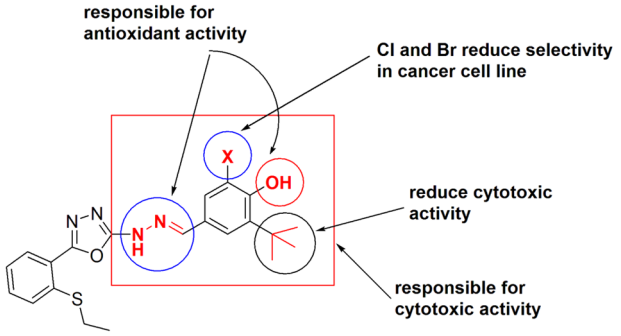

Fig. 5 The effects of various substituents toward antioxidant and cytotoxicity activity

compounds. Although compound **4e** is highly cytotoxic towards metastatic cancer cells, non-selectivity deter us from proceeding with this compound for further investigation of anticancer mechanism. Instead, we have selected the compound **4c** to demonstrate that it induces apoptosis through flow cytometry. This was accomplished by Annexin V-FITC/PI dual-staining assay of BxPC-3 cells after treatment with **4c** (13, 26, and 52 µM) for 72 h. Compound concentrations were selected based on the IC_{50} obtained previously. As illustrated in Fig. 3, a significant ($p < 0.01$) dose-independent increase from 15.00 to 47.20 % and finally to 46.33 % of apoptotic cells is observed (*right lower* and *upper* sections of the fluorocytogram), in contrast to the control which had only 1.7 %. This result is in a decreasing percent of viable cells from 96.97 % in control to 45.28 % in treated cells ($p < 0.01$) at the highest concentration tested. In a separate experiment, cell cycle arrest was demonstrated through flow cytometry by single-staining (PI) assay of BxPC-3 treated cells at time intervals of 24, 48, and 72 h. The cell cycle profiles and percent of each phase are shown in Fig. 4. Analysis of the DNA profiles revealed a significant ($p < 0.05$) time-dependent increase in cell populations at G0/G1 phase in comparison with control, displaying cell cycle arrest and suppression of cell proliferation. Taken together, both flow cytometry experiments show **4c** induce apoptosis with cell cycle arrest at G0/G1-phase; which is in agreement with the anticancer mechanisms reported for other derivatives of 1,3,4-oxadiazoles (Suan et al., 2013).

In relating the antioxidant and cytotoxic activities, parent compound **1**, containing only a 1,3,4-oxadiazole moiety, exhibited high DPPH radical scavenging activity, with an $IC_{50} = 2.22 \pm 0.01$ µg/mL, and did not show any cytotoxic potency in the tested cell lines. The same was observed regarding the cytotoxic potency of the intermediate compound **2**, which contains an ethyl ester moiety, and showed a FRAP value higher than the BHT positive control. Replacing the ester moiety in **2** with a hydrazide group in compound **3** enhanced the antioxidant activity, but with no notable change in the cytotoxic potency. This observation may be due to the presence of the free –NHNH2 group, the free electron pair of the NH2 does not participate in the resonance with the aromatic ring, thus it could act as an electron donor (Gozzo et al., 1999). Compounds **4a–e** are derivatives of compound **3**, formed after the introduction of the phenolic OH moiety with varying substitutions on the aromatic ring. Interestingly, the introduction of the phenolic OH confers cytotoxic potency against the tested cell lines, with the exception of compound **4d** (Table 3). It was reported that the phenolic OH moiety found in natural polyphenolic compounds, such as trolox and quercetin, is important towards suppressing ROS (Derochette et al., 2013; Priyadarsini et al., 2003). Because chronic inflammation from excessive ROS is one of the reasons for cancer development, suppressing it is a potential strategy for cancer therapy. Based on our antioxidant results, higher activity is observed for the phenolic compounds in DPPH than in the FRAP assay. Therefore, we infer that the scavenging activity of the reactive species by the compounds **4a–e** is caused by the phenolic OH moiety, which has hydrogen that can be donated. With regards to compound **4d**, the di-*tert*-butyl moiety flanking the phenolic OH may have caused steric hindrance to the hydrogen donating ability of this compound. Our structure–activity relationship data are summarized in Fig 5. These results indicate that 1,3,4-oxadiazole derivatives with phenolic OH and NH group have better scavenging activity, while in order to have cytotoxic activity, the 1,3,4-oxadiazole derivatives should contain a Schiff base group connected to a substituted benzene ring.

Conclusion

Eight new 1,3,4-oxadiazoles were synthesized and determined to have bioactive pharmacophores meeting the essential requirements for antioxidant and cytotoxic activities. The results revealed that compounds **1** and **3** showed strong antioxidant activities but display low cytotoxic potency. Oxadiazole derivatives **4a–e** showed variability in their antioxidant activities, and in addition to some cytotoxicity that could be due to the phenolic OH. The introduction of steric (di-*tert*-butyl) or electron withdrawing (Cl and Br) groups to the aromatic ring caused reduced potency and selectivity, respectively, in the cancer cell lines. Preliminary investigation of the anticancer mechanism for these compounds revealed compound **4c** induces apoptosis and causes cell cycle arrest at G0/G1 phase. Drug-likeness is observed in all of the compounds **1–4e**, based on the Lipinski and Veber rules, but poor human intestinal absorption was predicted with compound **4d** in Egan's model.

Acknowledgments The authors would like to thank the University of Malaya for UMRG grants (RP021B-14AFR), PPP grant (PG033-2012B), PRPUM grant (CG021-2013) and the Ministry of Higher Education of Malaysia grant (FP024-2014A) for supporting this study. The authors acknowledge CRYSTAL for providing the computational resources for computational intensive calculation and model building.

Compliance with ethical standards

Conflict of Interest The authors declare no conflicts of interest in this work.

References

Alam MS, Choi J-H, Lee D-U (2012) Synthesis of novel Schiff base analogues of 4-amino-1, 5-dimethyl-2-phenylpyrazol-3-one and their evaluation for antioxidant and anti-inflammatory activity. Bioorg Med Chem 20:4103–4108

Benzie IF, Strain J (1996) The ferric reducing ability of plasma (FRAP) as a measure of "antioxidant power": the FRAP assay. Anal Biochem 239:70–76

Bergström CA, Holm R, Jørgensen SA, Andersson SB, Artursson P, Beato S, Borde A, Mullertz A (2013) Early pharmaceutical profiling to predict oral drug absorption: Current status and unmet needs. Eur J Pharm Sci 57:173–199

Brand-Williams W, Cuvelier ME, Berset C (1995) Use of a free radical method to evaluate antioxidant activity. Lebensm Wiss Technol 28:25–30

Derochette S, Franck T, Mouithys-Mickalad A, Ceusters J, Deby-Dupont G, Lejeune J-P, Neven P, Serteyn D (2013) Curcumin and resveratrol act by different ways on NADPH oxidase activity and reactive oxygen species produced by equine neutrophils. Chem Biol Interact 206:186–193

Desai N, Bhatt N, Somani H, Trivedi A (2013) Synthesis, antimicrobial and cytotoxic activities of some novel thiazole clubbed 1, 3, 4-oxadiazoles. Eur J Med Chem 67:54–59

Egan WJ, Lauri G (2002) Prediction of intestinal permeability. Adv Drug Deliver Rev 54:273–289

Egan WJ, Merz KM, Baldwin JJ (2000) Prediction of drug absorption using multivariate statistics. J Med Chem 43:3867–3877

Ferrari E, Lucca C, Foiani MA (2010) Lethal combination for cancer cells: synthetic lethality screenings for drug discovery. Eur J Cancer 46:2889–2895

Fuchs-Tarlovsky V (2013) Role of antioxidants in cancer therapy. Nutrition 29:15–21

Gerhäuser C, Klimo K, Heiss E, Neumann I, Gamal-Eldeen A, Knauft J, Liu G-Y, Sitthimonchai S, Frank N (2003) Mechanism-based *in vitro* screening of potential cancer chemopreventive agents. Mutat Res 523:163–172

Gozzo A, Lesieur D, Duriez P, Fruchart J-C, Teissier E (1999) Structure-activity relationships in a series of melatonin analogues with the low-density lipoprotein oxidation model. Free Radic Biol Med 26:1538–1543

Hegazy GH, Ali HI (2012) Design, synthesis, biological evaluation, and comparative Cox1 and Cox2 docking of *p*-substituted benzylidenamino phenyl esters of ibuprofenic and mefenamic acids. Bioorg Med Chem 20:1259–1270

Hoelder S, Clarke PA, Workman P (2012) Discovery of small molecule cancer drugs: successes, challenges and opportunities. Mole Oncol 6:155–176

Husain A, Ahmad A, Alam MM, Ajmal M, Ahuja P (2009) Fenbufen based 3-[5-(substituted aryl)-1, 3, 4-oxadiazol-2-yl]-1-(biphenyl-4-yl) propan-1-ones as safer antiinflammatory and analgesic agents. Eur J Med Chem 44:3798–3804

Karadag A, Ozcelik B, Saner S (2009) Review of methods to determine antioxidant capacities. Food Anal Method 2:41–60

Kotaiah Y, Harikrishna N, Nagaraju K, Venkato RC (2012) Synthesis and antioxidant activity of 1, 3, 4-oxadiazole tagged thieno [2, 3-d] pyrimidine derivatives. Eur J Med Chem 58:340–345

Kundu JK, Surh Y-J (2012) Emerging avenues linking inflammation and cancer. Free Radic Biol Med 52:2013–2037

Lipinski C, Lombardo F, Dominy B, Feeney P (1997) Experimental and computational approaches to estimate solubility and permeability in drug discovery and development settings. Adv Drug Deliver Rev 23:3–25

Lipinski C, Lombardo F, Dominy B, Feeney P (2001) Experimental and computational approaches to estimate solubility and permeability in drug discovery and development settings. Adv Drug Deliver Rev 46:3–26

Looi CY, Moharram B, Paydar M, Wong YL, Leong KH, Mohamad K, Arya A, Wong WF, Mustafa MR (2013) Induction of apoptosis in melanoma A375 cells by a chloroform fraction of *Centratherum anthelminticum* (L.) seeds involves NF-kappaB, p53 and Bcl-2-controlled mitochondrial signaling pathways. BMC Complement Altern Med 13:166

Malich G, Markovic B, Winder C (1997) The sensitivity and specificity of the MTS tetrazolium assay for detecting the *in vitro* cytotoxicity of 20 chemicals using human cell lines. Toxicology 124:179–192

Nordberg J, Arnér ES (2001) Reactive oxygen species, antioxidants, and the mammalian thioredoxin system. Free Radic Biol Med 31:1287–1312

Omar F, Mahfouz N, Rahman M (1996) Design, synthesis and anti-inflammatory activity of some 1, 3, 4-oxadiazole derivatives. Eur J Med Chem 31:819–825

Petit J, Meurice N, Kaiser C, Maggiora G (2012) Softening the Rule of Five - where to draw the line? Bioorg Med Chem 20:5343–5351

Pospíšil J (1993) Chemical and photochemical behaviour of phenolic antioxidants in polymer stabilization: a state of the art report, part II. Polym Degrad Stabil 39:103–115

Prasad S, Gupta SC, Tyagi AK, Aggarwal BB (2014) Curcumin, a component of golden spice: From bedside to bench and back. Biotechnol Adv 32:1053–1064

Prior RL, Wu X, Schaich K (2005) Standardized methods for the determination of antioxidant capacity and phenolics in foods and dietary supplements. J Agr Food Chem 53:4290–4302

Priyadarsini KI, Maity DK, Naik GH, Sudheer KM, Unnikrishnan MK, Satav JG, Mohan H (2003) Role of phenolic OH and methylene hydrogen on the free radical reactions and antioxidant activity of curcumin. Free Radic Biol Med 35:475–484

Rapolu S, Alla M, Bommena VR, Ramalinga M, Nishant J, Venkata RB, Madhava RB (2013) Synthesis and biological screening of 5-(alkyl (1H-indol-3-yl))-2-(substituted)-1, 3, 4-oxadiazoles as antiproliferative and anti-inflammatory agents. Eur J Med Chem 66:91–100

Ren S, Wang R, Komatsu K, Patricia B-K, Yegor Z, Charles E, Csaba C, Zoltan A, Eric JL (2002) Synthesis, biological evaluation, and quantitative structure-activity relationship analysis of new Schiff bases of hydroxysemicarbazide as potential antitumor agents. J Med Chem 45:410–419

Revanasiddappa B, Subrahmanyam E (2009) Chloramine-T mediated synthesis of 1, 3, 4-oxadiazoles. Orient J Chem 25:707–710

Soobrattee MA, Neergheen VS, Luximon-Ramma A, Aruoma OI, Bahorun T (2005) Phenolics as potential antioxidant therapeutic agents: mechanism and actions. Mutat Res Fund Mol Mech Mut 579:200–213

Suan J, Li M-H, Qian S-S, Guo F-J, Dang X-F, Wang X-M, Xue Y-R, Zhu H-L (2013) Synthesis and antitumor activity of 1, 3, 4-oxadiazole possessing 1, 4-benzodioxan moiety as a novel class

of potent methionine aminopeptidase type II inhibitors. Bioorg Med Chem Lett 23:2876–2879

Tang JJ, Fan GJ, Dai F, Ding DJ, Wang Q, Lu DL, Ran RL, Zhou B (2011) Finding more active antioxidants and cancer chemoprevention agents by elongating the conjugated links of resveratrol. Free Radic Biol Med 50:1447–1457

Tang A, Lien EJ, Lai MM (1985) Optimization of the Schiff bases of N-hydroxy-N'-aminoguanidine as anticancer and antiviral agents. J Med Chem 28:1103–1106

Tung Y-T, Wu JH, Kuo YH, Chang ST (2007) Antioxidant activities of natural phenolic compounds from *Acacia confusa* bark. Bioresource Technol 98:1120–1123

Veber DF, Johnson SR, Cheng H-Y, Smith BR, Ward KW, Kopple KD (2002) Molecular properties that influence the oral bioavailability of drug candidates. J Med Chem 45:2615–2623

Vineis P, Wild CP (2014) Global cancer patterns: causes and prevention. Lancet 383:549–557

Wils P, Warnery A, Phung-Ba V, Legrain S, Scherman D (1994) High lipophilicity decreases drug transport across intestinal epithelial cells. J Pharmacol Exp Ther 269:654–658

Wu Y, Antony S, Meitzler JL, Doroshow JH (2014) Molecular mechanisms underlying chronic inflammation-associated cancers. Cancer Lett 345:164–173

Yehye WA, Abdul RN, Alhadi A, Khaledi H, Ng SW, Ariffin A (2012) Butylated hydroxytoluene analogs: synthesis and evaluation of their multipotent antioxidant activities. Molecules 17:7645–7665

Zhang M-Z, Mulholland N, Beattie D, Irwin D, Gu Y-C, Chen Q, Yang G-F, Clough J (2013) Synthesis and antifungal activity of 3-(1, 3, 4-oxadiazol-5-yl)-indoles and 3-(1, 3, 4-oxadiazol-5-yl) methyl-indoles. Eur J Med Chem 63:22–32

Zhang M-Q, Wilkinson B (2007) Drug discovery beyond the 'Rule-Of-Five'. Curr Opin Biotechnol 18:478–488